

TRABAJO DE FIN DE GRADO:

Usage of astronomical geodesy for millimetric ground deformation detection

Septiembre 2014

Autora:

Itahisa González Álvarez

Tutores:

M^a Jesús Arévalo Morales

Antonio Eff-Darwich Peña

Grado en Física

Curso 2013-2014

Abstract

La actividad volcánica lleva consigo algunos fenómenos potencialmente peligrosos, como terremotos, tsunamis, coladas de lava, nubes piroclásticas o deformaciones del terreno. Aunque algunos de estos fenómenos no son predecibles, sus consecuencias son tan importantes que la continua vigilancia y la detección temprana son esenciales para calcular y prevenir cualquier posible riesgo para las población.

La observación y detección de estos desplazamientos es esencial, ya que son uno de los síntomas más tempranos de la actividad volcánica, así como indicadores de fenómenos como los corrimientos de tierra. Por ello, proporcionan abundante información que puede ser de vital importancia a la hora de entender los procesos que ocurren en la litosfera y cuantificar los riesgos geológicos de estos fenómenos. Las magnitudes típicas de estos desplazamientos varían desde unos pocos milímetros hasta más de un metro en los casos más dramáticos. En la región de estudio, la isla de Tenerife, se monitorizan mediante estaciones GPS, interferometría de radar de apertura sintética (InSAR) y otros métodos geodésicos clásicos, todos ellos con una precisión de en torno a 1cm.

Así, con el fin de realizar mediciones de posibles deformaciones en el terreno, se ha diseñado un dispositivo que consta de una pequeña plataforma, un telescopio y un sensor CCD mediante el uso de la posición invariante del polo Norte celeste en el cielo. Aunque el método se aplicará principalmente a deformaciones debidas a causas volcánicas en la isla de Tenerife, la mayor de las Islas Canarias, podría ser aplicado también a aquellas ocurridas como consecuencia de otros mecanismos, como la presencia de aguas subterráneas, los deslizamientos de tierra en laderas, etc., por lo que podría ser de utilidad en multitud de campos.

A fin de poner a prueba el dispositivo, se llevó a cabo la simulación sobre el terreno de una serie de deformaciones del terreno de valores +1mm, +2mm y +3mm y se contrastaron las imágenes obtenidas para una posición de referencia del polo norte celeste, obteniendo así que es posible llegar a detectar por este método deformaciones del orden de 1mm.

Index

1. Aim of this work.....	4
2. Introduction.....	5
2.1. Geological setting.....	6
2.2. Ground deformations.....	8
2.3. The North Celestial Pole.....	8
3. Crustal deformation detection methods: state-of-the-art.....	10
4. Methods and materials.....	12
4.1. Expected values.....	12
4.1.1. Dikes.....	13
4.1.2. Magma chamber.....	17
4.1.3. Fault.....	19
4.2. Design.....	20
4.3. Methodology.....	21
5. Preliminary results.....	23
6. Conclusions and future works.....	26
REFERENCES.....	29

1. Aim of this work.

El objetivo de este trabajo es detectar deformaciones milimétricas y submilimétricas del terreno mediante el diseño de un dispositivo que permita la simulación de tales fenómenos y el establecimiento de una metodología barata y robusta mediante la cual sea posible analizar y realizar predicciones sobre los resultados obtenidos.

The goal of this work is to implement a cheap and robust methodology to detect millimetrical and submillimetrical ground deformations by using stellar cartography. In particular, this work is intended to the following:

- To establish an estimate magnitude to the expected crustal deformations due to volcanic activity in the island of Tenerife.
- To design a specific device to simulate and obtain ground deformation data by using the position of the north celestial pole on the sky.
- To implement a predictive and cheap methodology to analyse the data the previous device collects and infer the magnitude of crustal deformations from them.

2. Introduction.

Tenerife es la mayor de las islas del archipiélago canario, así como una de las islas volcánicas más grandes del mundo. A pesar de que la última erupción registrada en esta isla data de 1909, algunos signos evidencian la presencia hoy en día de actividad volcánica, como las fumarolas en el cráter del Teide, las emisiones de gases difusos o la elevada temperatura de las aguas subterráneas. La monitorización constante de estos fenómenos es de vital importancia, por lo que es conveniente prestar especial atención a los síntomas tempranos de la actividad volcánica. En este trabajo se analizarán en particular las deformaciones del terreno asociadas al volcanismo de la isla de Tenerife, definidas como desplazamientos del terreno con respecto a una posición de referencia, ya sean horizontales o verticales. Cuantificar la magnitud de estos movimientos es esencial, ya que proporcionan abundante información que puede ser crucial a la hora de entender e interpretar los procesos dinámicos que se producen en la litosfera y, así, delimitar los riesgos geológicos asociados.

La astronomía, y particularmente la cartografía celeste, ha sido de gran utilidad para los seres humanos desde la antigüedad y se ha empleado en ámbitos tan dispares como la navegación o la agricultura. La estrella Polar, por ejemplo, ha servido durante siglos para conocer la dirección del norte. En este trabajo, sin embargo, no se empleará esta estrella, sino que se hará uso de la posición del polo norte celeste, siendo éste el punto del cielo en el que el eje de rotación de la Tierra corta a la esfera celeste en su hemisferio septentrional. Éste, junto con el polo sur celeste, constituyen los únicos puntos auténticamente invariantes del cielo, por lo que es posible usarlos como guía o referencia.

The position of the stars in the sky has always been used to make different kinds of calculations. The North Star, defined as the nearest star to the North celestial pole, which corresponds to Alpha Ursae Minoris in modern times, is a good example. It has been used since ancient times to find the direction of north, as well as to calculate latitudes. Besides this, the careful observation of the firmament was essential in navigation or agriculture, making it possible to obtain very important calculations such as the passing of time, positions or the route when going from one place to another.

2.1. Geological setting.

Tenerife is the largest island of the canarian archipelago, as well as one of the largest volcanic islands in the world. It is located between latitudes 28-29° N and longitudes 16-17° W, 280 km distant from the African coast. The age of this volcanic region varies from Middle Miocene to present, with no evidence of important gaps in its volcanic activity history, at least in the last 3 to 4 Ma (Ancochea et al., 1990, 1999). This activity is still evident in stationary low temperature fumarolic activity at Teide crater, diffusive gaseous emissions (Valentín et al., 1990; Albert-Beltrán et al., 1990; Hernández et al., 1998; Pérez et al., 1996), groundwater temperatures reaching up to 50°C and volcanic contamination of groundwater in the subsurface of the central region (Bravo et al., 1976; Carracedo and Soler, 1983; Farrujia et al., 1994).

The morphology of Tenerife is the result of a long and complex geological evolution: the subaerial part of the island was formed after a series of fissural eruptions of ankaramite, basanite and alkali basalts that occurred between 12 and 3.3 Ma (Ancochea et al. 1990, Araña et al. 2000, Guillou et al. 2004) and left three eroded massifs, resulting from the erosion of the original shield volcanoes, occupying the three corners of the island (Teno, Anaga and Roques del Conde massifs). In the central part of the island, the emission of basalts and differentiated volcanics from 3.5 Ma to present gave rise to a large central volcanic complex, the Las Cañadas Edifice (Martí et al, 1994). After a period of mafic volcanism, several periods of phonolitic activity took place, culminating in the formation of a large elliptical depression measuring 16x9 km², known as Las Cañadas Caldera. In the northern sector of the caldera appears the Teide-Pico Viejo complex, a large stratovolcano that has grown during the last 175 Ky, as a product of the most recent phase of central volcanism. The post-shield basaltic activity, which overlaps the Las Cañadas Edifice, is mainly found on two ridges (NE and NW), which converge on the central part of the island (Ancochea et al. 1990; Carracedo, 1994; Ablay and Hurlimann, 2000). Large scale lateral collapses, involving rapid mass movements of hundreds of cubic kilometres of rock, are responsible for the formation of three valleys: La Orotava, Güimar and Icod. Recorded eruptive activity has consisted of six strombolian eruptions (Cabrera and Hernández-Pacheco, 1987), namely Siete Fuentes (1704), Fasnia (1705), Arafo (1705), Arenas Negras (1706), Chahorra (1798) and Chinyero (1909). The last three eruptions occurred at the NW axis system, the most active area of the island together with El Teide-Pico Viejo Edifice for the last 50,000 years (Carracedo et al. 2003a, 2003b).

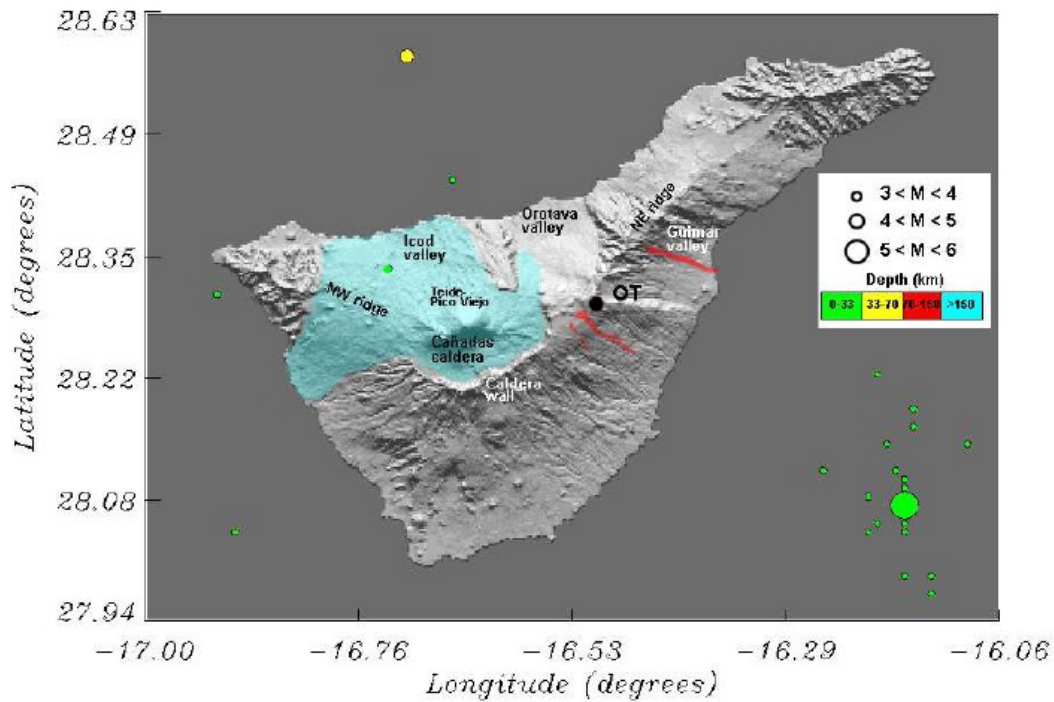


Figure 1. Simplified shaded-relief map of the island of Tenerife, indicating the most important geological features (see text for details). The light blue and red areas indicate the regions affected by recent (last 10 ka) and historical (last 500 years) volcanic activity, respectively. The location of El Teide observatory (OT) is indicated by a black filled circle, whereas filled circles of different sizes and colours indicate the location, magnitude and depth of the earthquakes registered during the period 1973-2008. (Extracted from Eff-Darwich et al, 2009)

It is important to mention, in the context of geodetic monitoring, the possible existence of a shallow magma chamber underneath the Teide-Pico Viejo complex. It is estimated from petrologic analyses (Araña 1985; Araña et al. 1989) that the top of the magma 5 chamber is located at sea level, having a volume of approximately 30 km³ and a radius of 2 kilometres (under the supposition of spherical shape). Thermodynamical (Diez and Albert 1989) and chemical (Albert-Beltrán et al. 1990) modeling of the fumaroles at El Teide summit revealed that the present temperature at the surface of the magma chamber would be approximately 350°C, whereas the top of the chamber coincides with that calculated from petrologic analyses. However, Araña et al. (2000) found long-wavelength magnetic anomalies in the central part of Tenerife that could be interpreted as the top of deep intrusive bodies or magma chambers zone (≈ 5.7 km b.s.l.). In this sense, the possible location of the top of the magma chamber ranges from sea level to nearly 6 kilometres below sea level. It is also important for geodetic studies that most recent eruptions (< 3 Ma) have been fed by dikes (Fernández et al. 2003). These dikes are associated to systems of deep fractures that generally respond to

regional tectonics. In other cases, the dikes are located in shallow radial or circular fractures in large volcanic structures. Most of the visible dikes are less than one meter thick in the shallowest sections. However, when erosion exposes deeper sections, they are seen to be much thicker, especially those of a saline composition. Regional fractures in Tenerife are mainly to be seen in the two ridges (NE and NW) that converge in the central region of the island. There are also major radial fractures associated to the eruptive systems of the Teide-Pico Viejo volcano, in the central area of Tenerife.

2.2. Ground deformations.

Crustal deformations are defined as ground displacements respect to its original position. These movements can be both horizontal or vertical and their causes vary: from ground slides due to instability or ground settlement to movements due to earthquakes, volcanic activity or even the presence of underground water flows. Analysing and observing these deformations, either by using GPS stations, Synthetic Aperture Radar interferometry (InSAR) or some other method are essential, as they constitute an early indicator of major phenomena like landslides or volcanic eruptions and, therefore, they provide abundant information which can be crucial when trying to understand of the dynamic processes produced within the lithosphere and quantifying geological hazards.

Along this work, crustal deformations will be analysed, specially those resulting from volcanic activity in Tenerife. The surface around a volcanically active area is deformed before, during and also after that activity as a consequence of volcanic eruptions and the evolution of the different associated phenomena. Quantifying the magnitude of these changes constitutes a useful way of detecting early symptoms of eruptions, as they can be detected and measured shortly after magma starts its way up and long before it reaches the ground level, thus improving the volcanic monitoring and helping preventing any possible damage to the population in the area around the volcano.

2.3. The North Celestial Pole.

The Celestial Poles are imaginary dots on the sky where the Earth's rotation axis crosses the celestial sphere, thus existing two of them, named the North Celestial Pole (NCP hereafter) and the South Celestial Pole (SCP). As a result of the Earth's rotation, every star of the celestial sphere appears to rotate around these spots with a 24 hours period, while they remain static. Actually, both

the NCP and the SCP experience a slow change in their positions due to the precession of the equinoxes, which makes the Earth's rotation axis trace small circles over the celestial sphere. However, this movement has a period of about 26,000 years which makes it absolutely imperceptible in the time scales relevant for this work (typically from months to years).

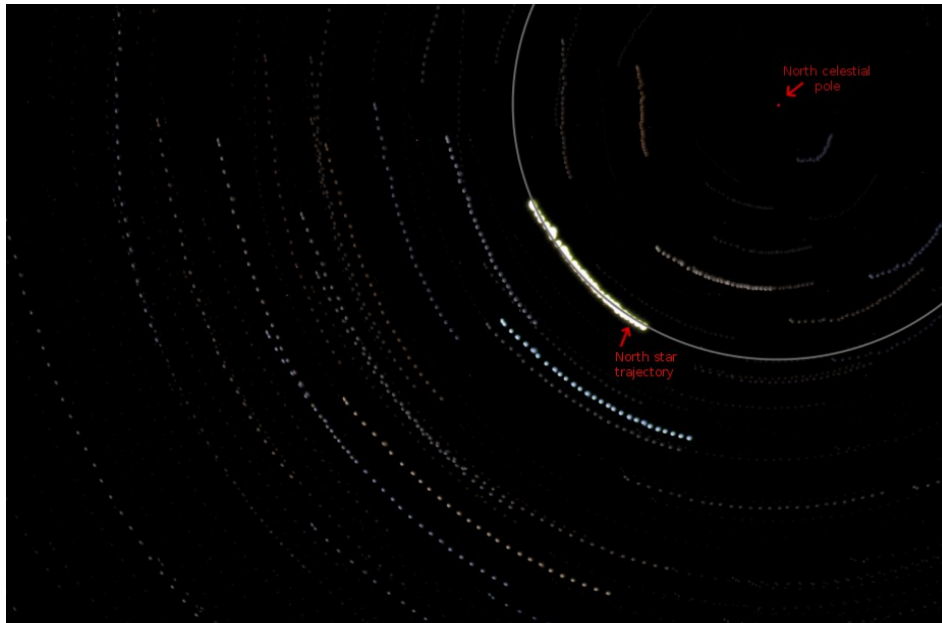


Figure 2. Overlap of a photographic series of the area around the North pole. The composition shows the continuous movement of the stars around the NCP.

Alpha Ursae Minoris, also known as the North Star or Polaris, is located near the NCP, slightly displaced from it at so short a distance that its movement around it goes unnoticed to the naked eye. In order to illustrate the displacement of Polaris from the NCP, 36 photographs of the area around it were taken and overlapped, as displayed in figure 2. These images, with an exposure time of 30 seconds were taken for 3 hours at intervals of 5 minutes with a Canon EOS 40D reflex camera with a Tamron 200-500 F/5-6.3 lens settled to 500mm, ISO 640 and f/8, being the whole device mounted on a tripod to ensure stability and avoid unwanted movements. The result shows how the North Star, together with the rest of the stars present on the photographs, describes a circle around an apparently empty area. The stars trajectories will allow us to estimate the NCP's position as well as the device's accuracy.

3. Crustal deformation detection methods: state-of-the-art.

La monitorización de las deformaciones del terreno en la isla de Tenerife se basó, a finales del s. XX, en una microrred geodésica situada en el interior de la caldera de Las Cañadas. Sin embargo, tras detectarse movimientos del terreno mediante técnicas InSAR fuera de la zona de control se llevó a cabo un estudio que estableció la conveniencia de extender la vigilancia al resto de la isla, con especial observación de aquellas zonas en las que se detectaron estos desplazamientos. Así, se estableció en la isla una red con 22 estaciones GPS que confirmó los resultados obtenidos previamente mediante InSAR. En la actualidad, existen dos redes de GPS instrumental operativas: una con 5 estaciones perteneciente al Instituto Geográfico Nacional (IGN) y otra con 11 estaciones del Instituto VOLcanológico de CANarias (INVOLCAN).

Las Islas Canarias, además, cuentan con un cielo nocturno de gran calidad, lo que ha hecho que se instalen en ellas dos observatorios astronómicos de relevancia mundial, el del Teide en Tenerife y el del Roque de los Muchachos en La Palma. Estos observatorios han sido, asimismo, de utilidad en la monitorización de los fenómenos volcánicos, al contribuir con productos secundarios de las observaciones astrofísicas, como los datos de precisión en el apuntado de los telescopios.

Crustal deformation monitoring in Tenerife was based, until the last decade of the 20th century, on a geodetic micro-network located at Las Cañadas caldera. However, two unexpected ground movements located out of the control area and detected by InSAR techniques and a series of sensitivity proofs showed the convenience of extending the network to the rest of the island (Fernández et al. 2003). Thus, a 22 GPS stations network was settled around the island, arranging stations more densely to enforce surveillance around the areas where some deformations were detected. This new network confirmed the previous InSAR results as well as the necessity of monitoring the entire island instead of just those areas close to Las Cañadas caldera.

Moreover, the presence of two astrophysical observatories in the islands has proven useful for crustal deformation studies as some secondary products from astrophysical observations, like telescopes pointing accuracy data, which must be in the order of the optical aberration introduced by the atmosphere in astronomical observations, could contain information on this topic that may complement the data collected from geodetic techniques. In this manner, tilting motions of the telescopes or of the buildings containing them, which include those due to structural effects, thermal deformation and geological activity, must be carefully monitored, as they must be smaller than the above mentioned optical aberration. An example of this kind of surveillance are the four tiltmeters

installed within the Themis solar telescope building, sited at El Teide observatory, which were considered a useful complement for the monitoring of the volcanic activity in the island after an analysis of the tilting data they collected from 1997 to 2006 (Eff-Darwich et al., 2008).

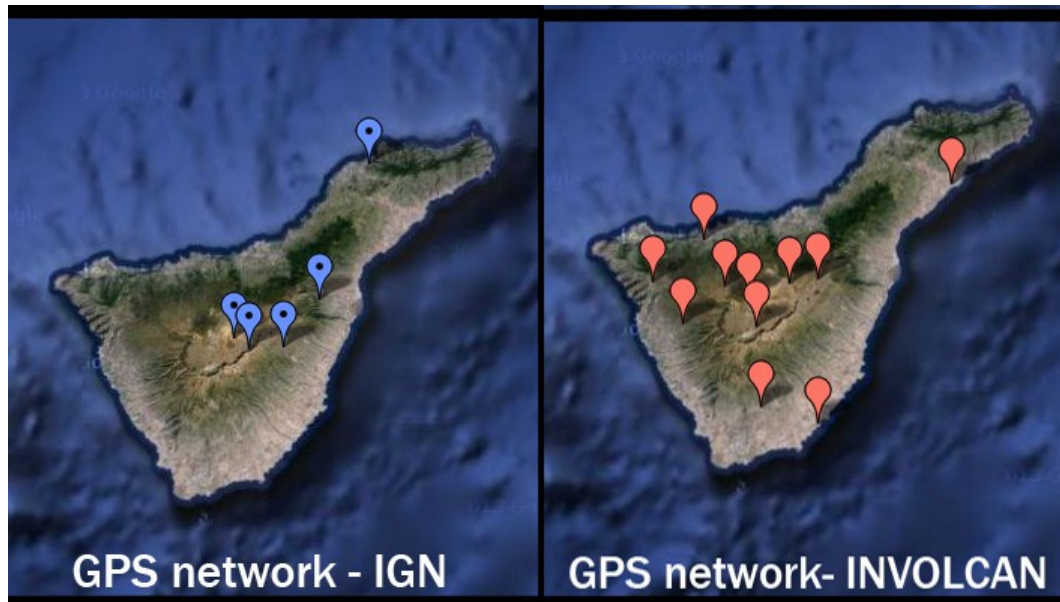


Figure 3. Operative GPS networks in Tenerife.

Currently, two different and permanent instrumental GPS networks operate in Tenerife island within the framework of a geodetic program for volcanic surveillance in the archipelago: the first one consists on five stations and is controlled by the National Geographic Institute (IGN); the second network, with eleven stations arranged around the island, is part of the volcanic monitoring carried out by the Technological Institute for Renewable Energies (ITER). These networks allow crustal deformation measurements with an accuracy up to 1 centimeter. In addition to them, synthetic aperture radar interferometry (InSAR) is also used to complete the crustal deformation studies in the island, reaching a similar accuracy of 1 centimeter, thus becoming a valuable complement to the rest of the monitoring techniques, as it allows to observe areas which are not regularly checked in addition to those which are already surveyed by the GPS networks, naturally limited by the necessary separation among stations.

4. Methods and materials.

En primer lugar, se empleó el software Mirone para realizar una serie de simulaciones de deformaciones del terreno como consecuencia de distintos tipos de actividad volcánica. En particular, se analizó el efecto de la inyección de magma en la cámara magmática del Teide, variando los parámetros para obtener diferentes volúmenes de la misma; la intrusión de magma a través de diques con distintas inclinaciones que quedan a distintas profundidades sin llegar a salir a la superficie y, por último, la deformación experimentada tras un desplazamiento de la falla que se postula que existe entre las islas de Tenerife y Gran Canaria. Estos valores permitieron estimar los valores de deformación a esperar en la isla de Tenerife.

A continuación, se llevó a cabo el planteamiento del dispositivo a emplear para realizar la simulación de estas deformaciones sobre el terreno. Así, empleando un telescopio buscador Orión 9x60, una cámara CCD Imaging Source DBK41AU02.AS y una plataforma en forma de cuña diseñada específicamente con este propósito, se obtuvo un instrumento cuyos componentes se encuentran fijados de manera permanente (eliminando así cualquier posible grado de libertad) y que apunta constantemente hacia el polo norte celeste (PNC).

Esta falta de posibles variaciones en las posiciones de los distintos elementos del dispositivo es precisamente la fortaleza del diseño y la base del método experimental propuesto, ya que de esta manera, tras su instalación, el campo visual de la CCD será siempre el mismo (el que está en torno al PNC), salvo en el caso de que sea el propio suelo sobre el que se asienta el instrumento el que se mueve. Con esto, se busca encontrar la correlación entre el valor de deformación del terreno y la desviación del PNC con respecto a su posición original en la imagen tomada por la CCD, estableciendo así un método de detección de desplazamientos del terreno a partir de la cartografía celeste.

4.1. Expected values.

The first step to analyse crustal vertical deformation is to obtain the expected values of this magnitude for the different deformation sources present in the region of study. For this purpose, we carried out a theoretical analysis to infer the ground deformation, in terms of ground tilt, associated

to a dislocation induced by a fault between Tenerife and Gran Canaria, a magma injection into the magmatic chamber of Teide and a magma intrusion through different dikes. Following Feigl and Dupré (1999), we specified a set of six parameters describing the rectangular fault patch: length, width, depth (and, indirectly, depth to top distance (DTT)), dip and slip on the fault plane vector (u_1 , u_2 , u_3) (see figure 4 for details). The chosen values for all these parameters are all typical values for the analysed phenomena.

Absolute vertical displacements and ground tilts associated to the fault dislocations were calculated (in mm) through the Mirone software developed by J.F. Luis (1999) based on the RNGCHN software, by Feigl and Dupré (1999). RNGCHN formulation approximates the surface movements produced by earthquake faulting or volcanic intrusion and generates the displacement components as the program's output.

These simulations were carried out on a portion of a global 30 arc-second map which combined bathymetric and digital elevation model data provided by the General Bathymetric Chart of the Oceans (GEBCO) from the British Oceanographic Data Centre (BODC). The position of the observatory has been marked in all figures and maps with 'OBS'.

4.1.1. Dikes.

Dikes are, in a geological context, flat bodies of rock that cut through a different kind of rocks at a different angles than the rest of the structure. They usually intrude on fissures between rocks, pushing everything they find on they way up to the sides.

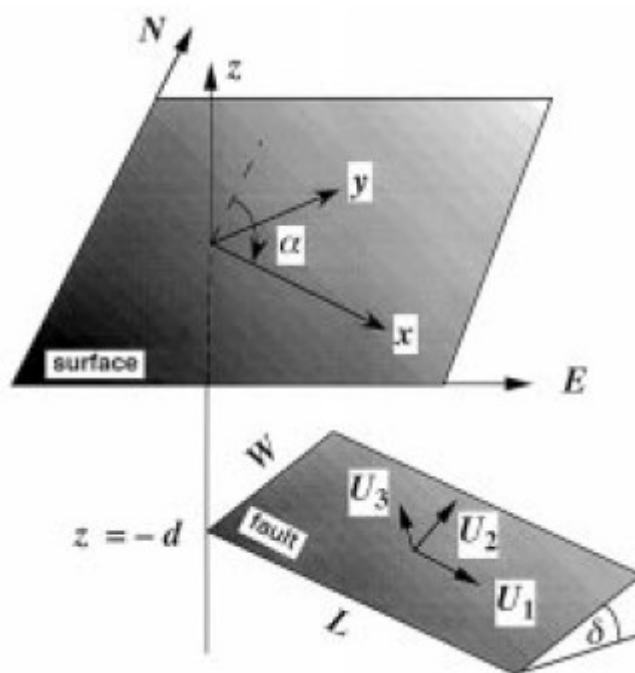


Figure 4. Fault geometry and symbols. Slip vector $U=[U_1, U_2, U_3]$ represents movement of hanging wall with respect to footwall signed such that positive U_1 is left-lateral strike slip, positive U_2 is thrusting dip slip, and U_3 is tensile slip.

(Extracted from Feigl and Dupré, 1999).

Two different dip angles, 70° and 90° , were simulated for a single dike located in the NE ridge with Mirone, as most part of the eruptive activity in the island for the last 50,000 years has occurred there. Figure 5 shows the surface projection of the simulated dikes (the maps on the forthcoming sections also show this projection instead of the actual position of the faults and dikes), which was chosen after considering that most eruptions involving dikes took place in that area, but it is to be noted that the effect of such phenomena at the observatory would depend greatly on the distance between them (the closer to the observatory, the stronger the effects). Besides that, different values of the depth to top distance (DTT) were applied to each case in order to analyse the cases of a dike extending from the mantle (around 40 km deep) to 5 m, 50 m and 500 m from the surface, so a total amount of six simulations were carried out for these tensional dislocations, all of them having a typical slip vector $(0, 0, 1000)$ (in mm).

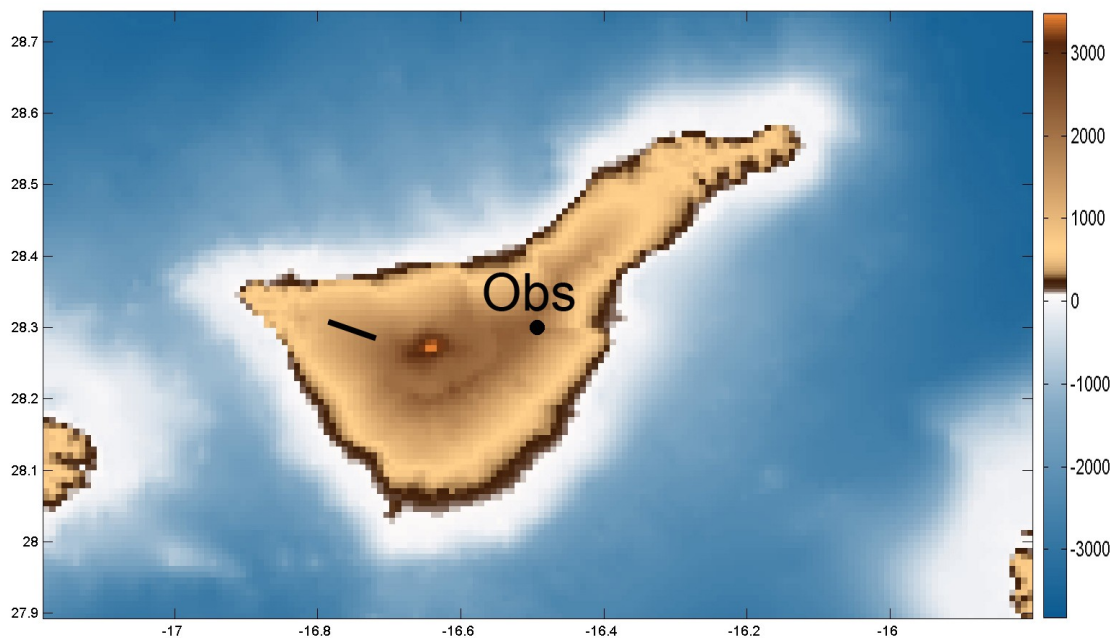


Figure 5. Locations of the simulated dike on the bathymetric-digital elevation model map. The colorbar at the side shows different colours for each height/depth.

Figures 6, 7, 9 and 11 show the deformation distribution obtained for each case as well as the expected deformation values at Teide observatory (all distances are expressed in millimeters). These values were obtained from the cross-section corresponding to the observatory's latitude of the deformation patterns. In this manner, the curves showed on the right column present the displacement values along the same latitude together with a vertical line to mark the position of the observatory and a horizontal trace to relate this position with its associated deformation value.

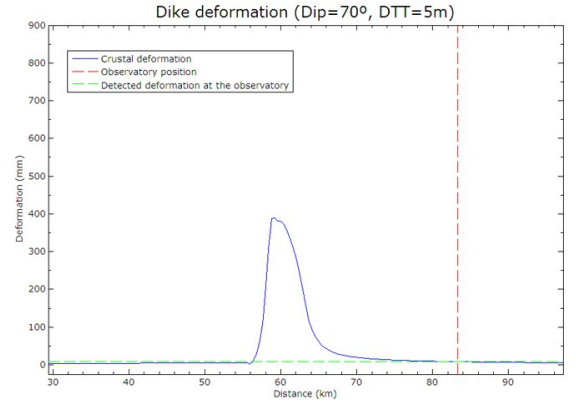
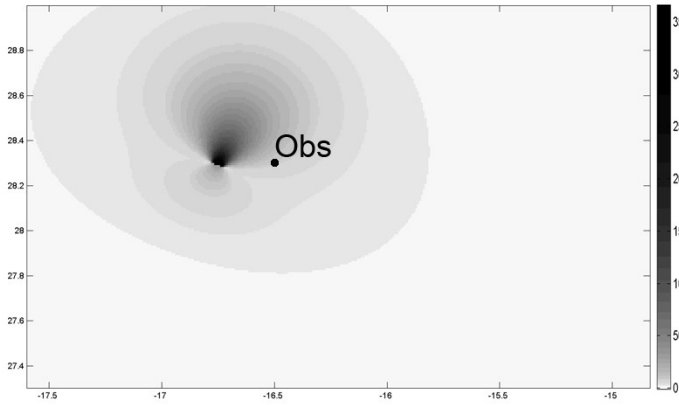
Dip = 70°

DTT

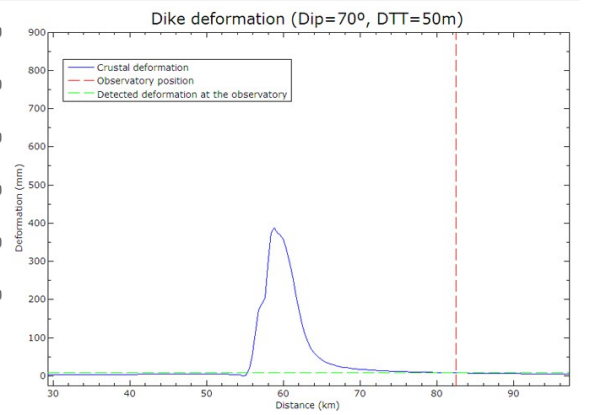
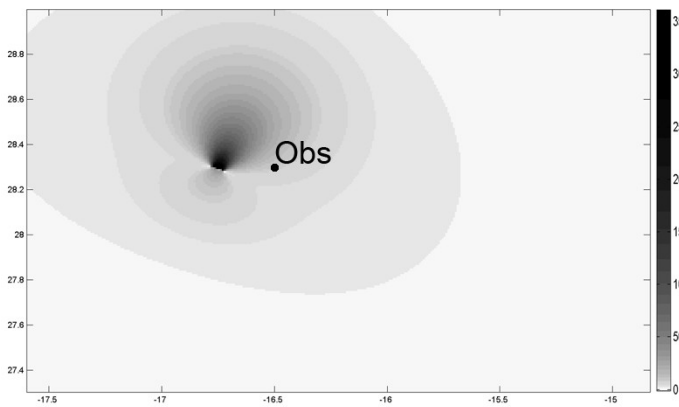
Deformation pattern (mm)

Expected value at the observatory

5 m



50 m



500 m

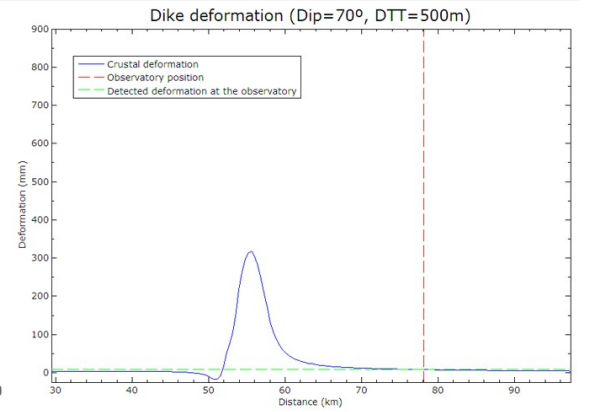
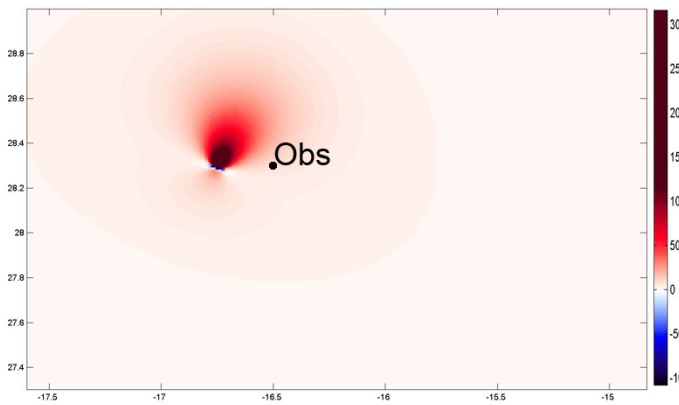


Figure 6. Effects of a 70° angled dike injection.

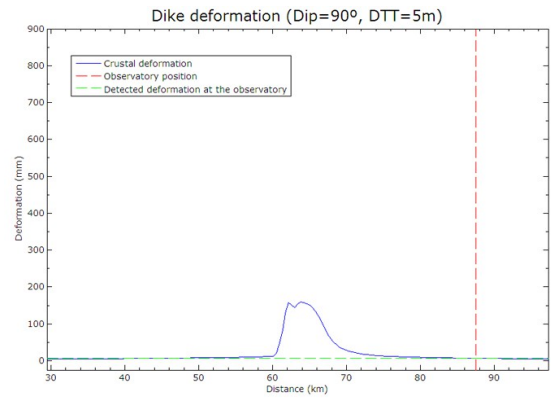
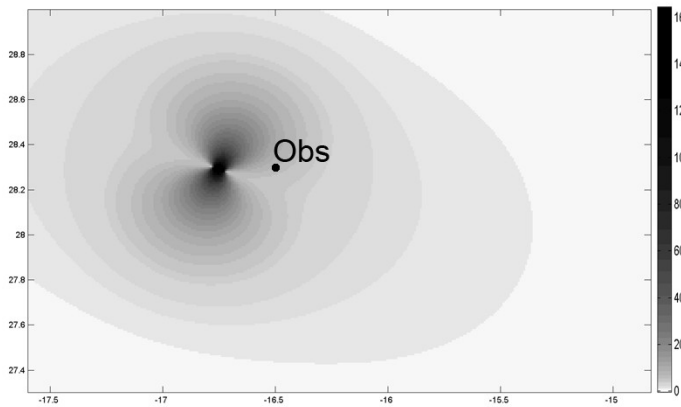
Dip = 90°

DTT

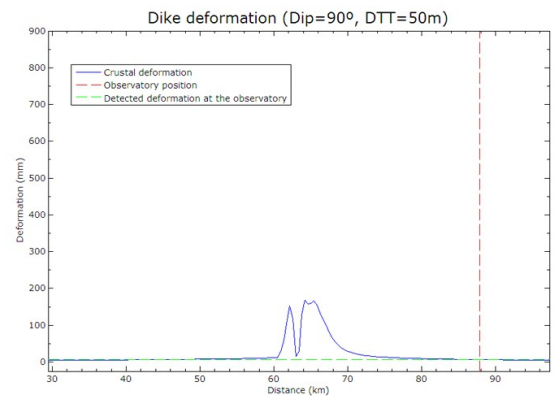
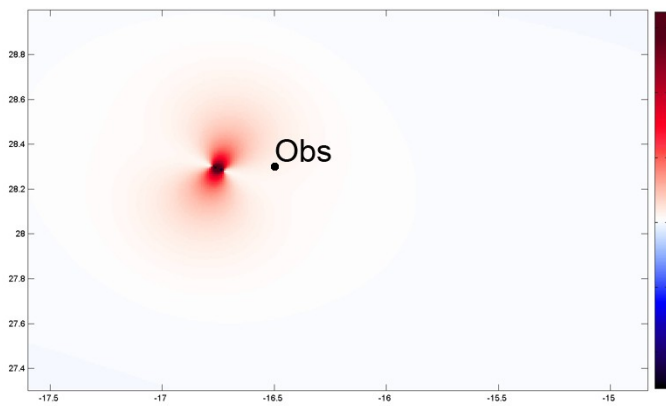
Deformation pattern (mm)

Expected value at the observatory

5 m



50 m



500 m

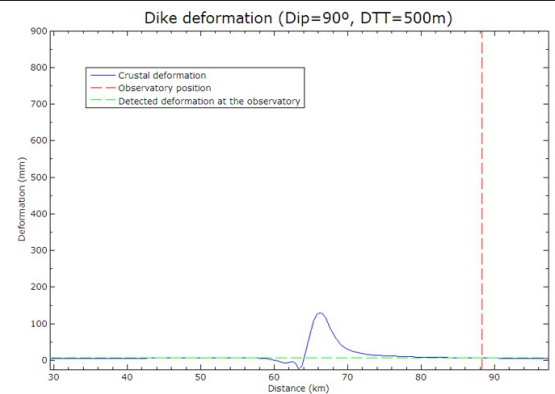
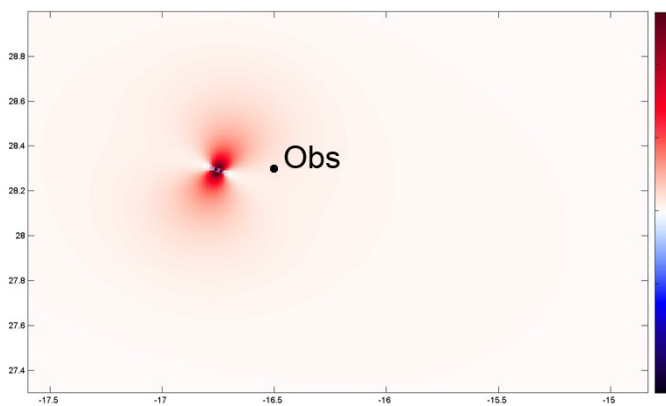


Figure 7 Effects of a 90° angled dike injection.

The results in figures 6 and 7 present similar deformation patterns in all cases. The expected displacements at the observatory for those dikes with dip angle of 70 degrees range from 8.0003 mm to 8.1827 mm, with a mean value of 8.0966 mm. For dikes with dip equals to 90 degrees, these values vary from 6.3613 mm to 6.7025 mm, with an average of 6.5601 mm. The total average deformation for the analysed dikes is 7.3284 mm at the observatory.

4.1.2. Magma chamber.

A magma chamber is a usually large underground reservoir of magma located under a volcano. As it was already mentioned, the possible location of the magma chamber underneath El Teide-Pico Viejo stratovolcano is unclear, ranging the position of the top of the chamber from approximately sea level to 6 kilometers below sea level.

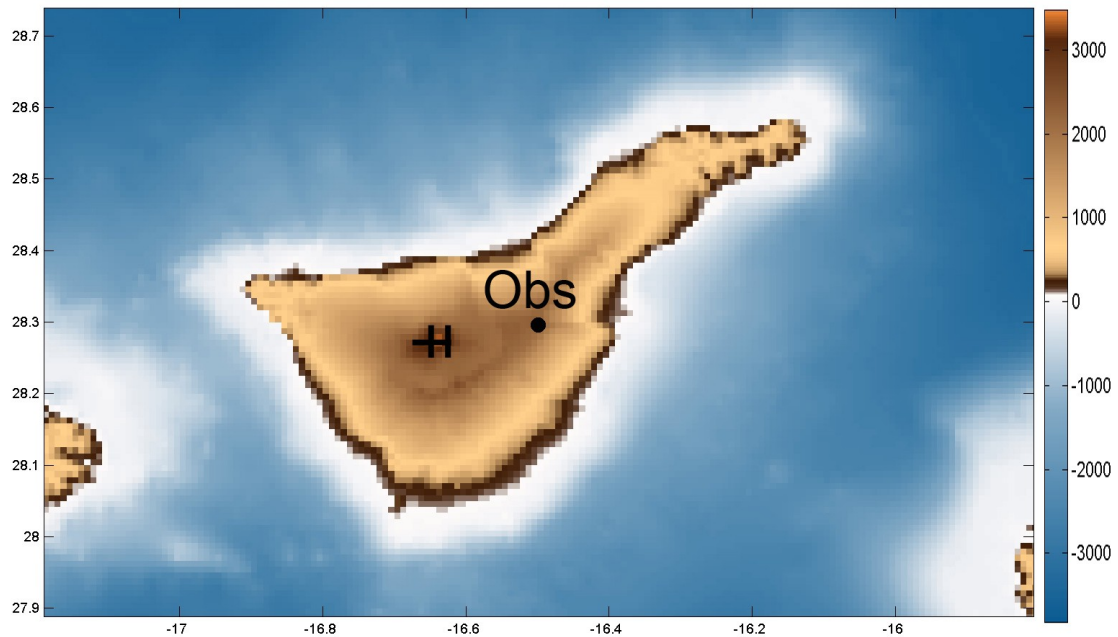


Figure 8. Situation of the simulated magma chamber.

The second case to be studied was a reactivation in the magmatic system associated to this volcano. As there is no simple way to simulate a magma chamber, specially when so many of its characteristics and parameters remain unknown, it was decided to use three independent perpendicular faults of the same length (around 5 km) and width (also 5 km) but different fault and geometrical parameters in order to model a spheroid. Two of these faults have a vertical disposition (dip=90°) while the third one lays horizontally (dip=0°) 4.5 km below the sea level. This way, the top and the bottom of the simulated magma chamber would be 2 km and 7 km below the sea level respectively. In addition to this, three different values of the tensile component of the slip vector, u_3 were applied to each case so that different magnitudes of this reactivation would be analysed. Figure 9 shows the deformation patterns obtained for each case as well as the estimated ground displacement at the observatory.

Magma chamber

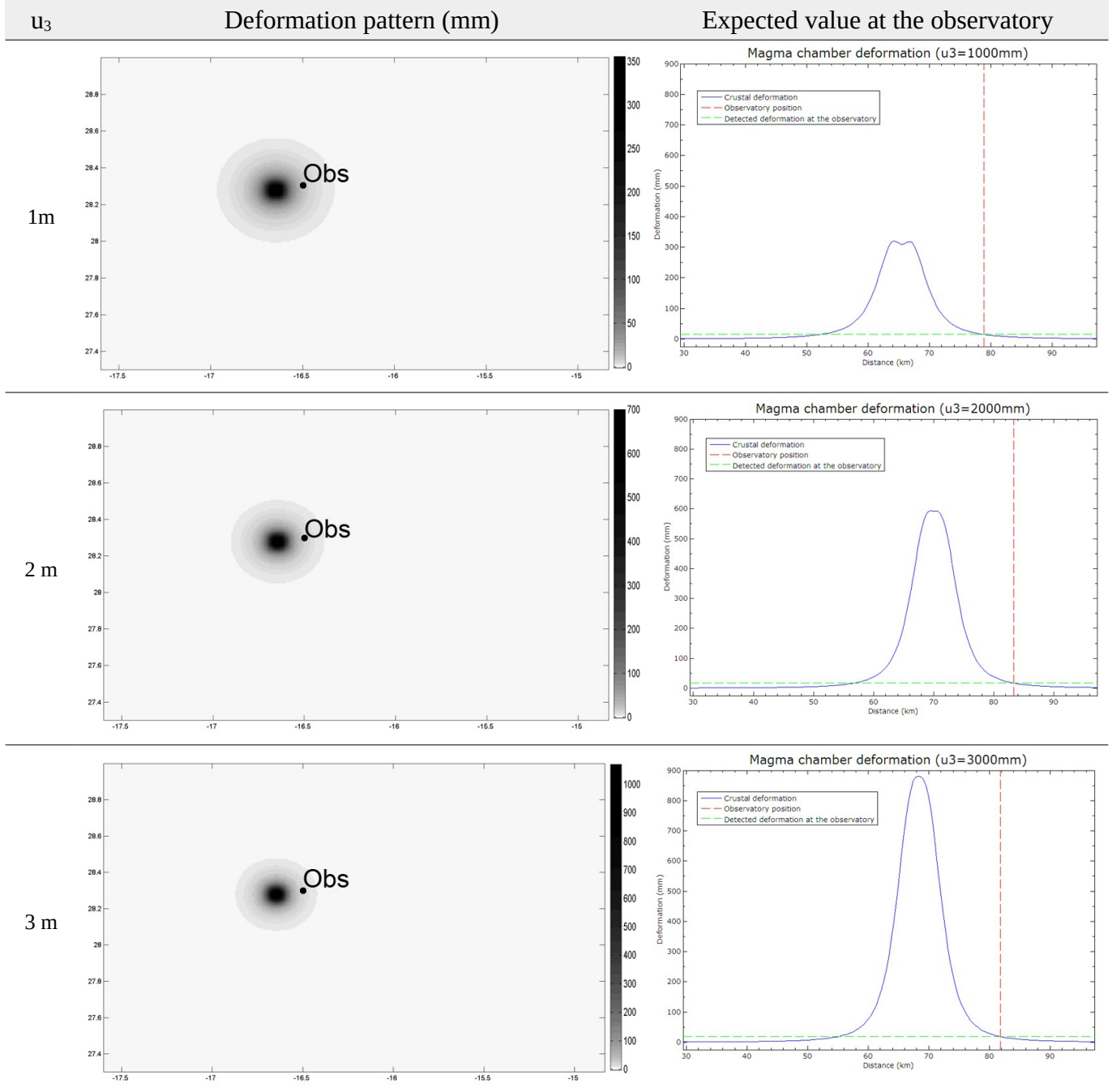


Figure 9. Effects of a reactivation on the magma chamber of the Teide-Pico Viejo complex.

Again, the deformation patterns are very similar for the analysed cases but the magnitude of the displacements differs, ranging their maximum values from 350 mm to 1000 m in the $u_3=1000$ mm case but these values are considerably smaller at the observatory, with 14.5032 mm, 16.9177 mm and 18.5787 mm for 1 m, 2 m and 3 m of tensile component of the slip vector respectively. The total average deformation at the observatory was estimated in 16.6665 mm.

4.1.3. Fault.

The third case in our theoretical analysis is represented by a dislocation induced by a postulated major NE-SW submarine fault parallel to the eastern coast of Tenerife. In 1989, a notorious earthquake ($M=5.2$) took place between Gran Canaria and Tenerife and it is assumed that it was caused by a dislocation originated within this fault (Eff-Darwich et al, 2008).

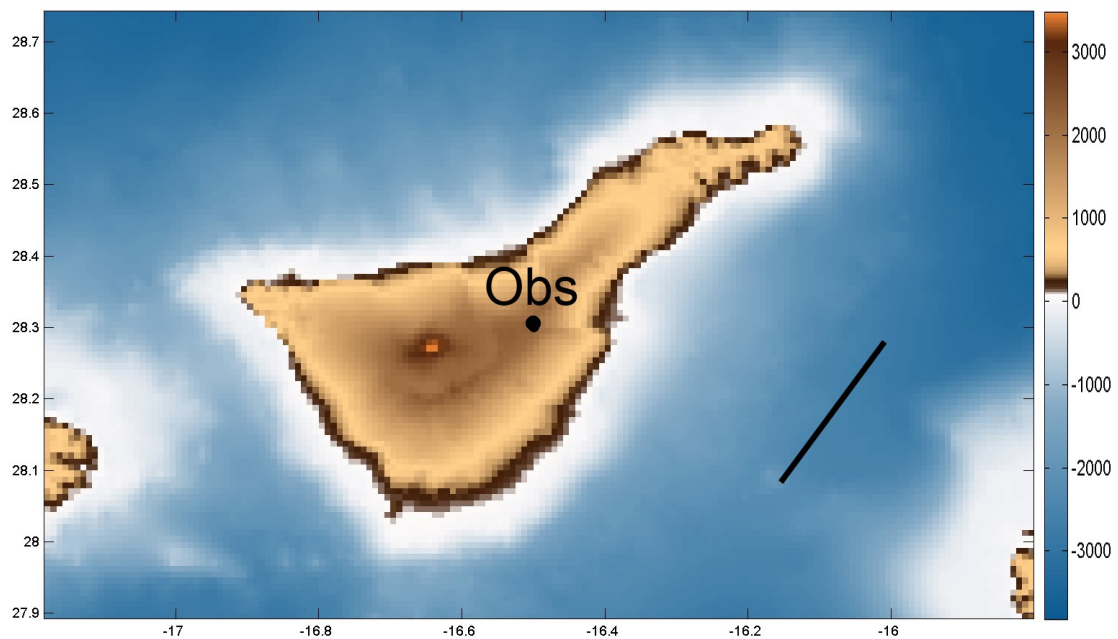
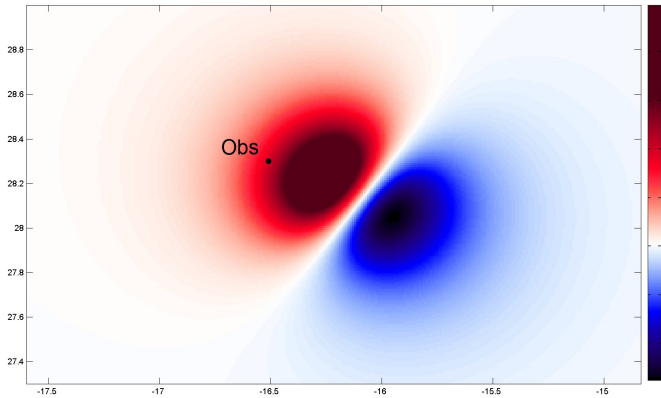


Figure 10. Localization of the major submarine fault that assumedly caused a 5.2 magnitude earthquake in 1989.

The selected values for the fault parameters were chosen in order to simulate an earthquake similar to the one happening in 1989. For this reason, the fault parameters were set to dip of 80 degrees, depth 40 km, length 30.883 km and the geometrical parameters correspond to a slip vector $u=(0, 250, 0)$ mm. Figure 10 presents the localization of the mentioned fault on the map and figure 11 shows the effects of the dislocation. In this case, the maximum magnitude of the crustal deformation is 9.1737 mm, thus being slightly larger than those obtained for dikes. The expected value at the observatory is 0.0692 mm.

Submarine fault

Deformation pattern (mm)



Expected value at the observatory

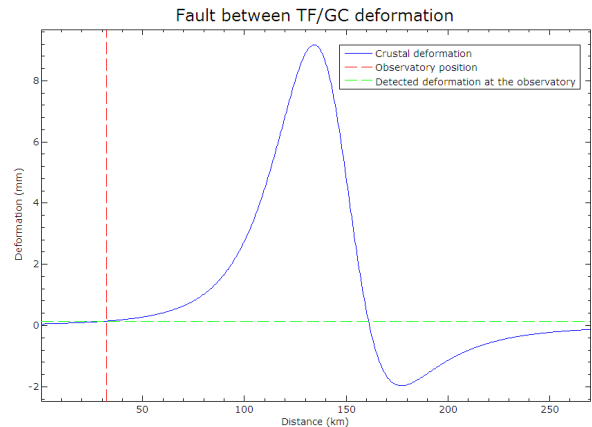


Figure 11. Deformation pattern and expected displacement at the observatory.

4.2. Design.

The unchanging position of the NCP on the firmament, as established in section 2.3., allows to use it as a guide or a reference. Consequently, a device consisting on a Orion 9x60 finder telescope, an Imaging Source CCD camera (model *DBK41AU02.AS*) and a 28° (mean latitudinal angle for Tenerife) angled platform as a base has been designed in order to make it possible to simulate crustal deformations and measure their effect on the visual field of the device, whose axis is permanently pointing north. In this manner, the telescope is directed to the NCP at all time, as showed in figure 12. A tripod or a stable base on the ground with a series of slots that allow fixing the device to them are used to establish the position of the instrument.

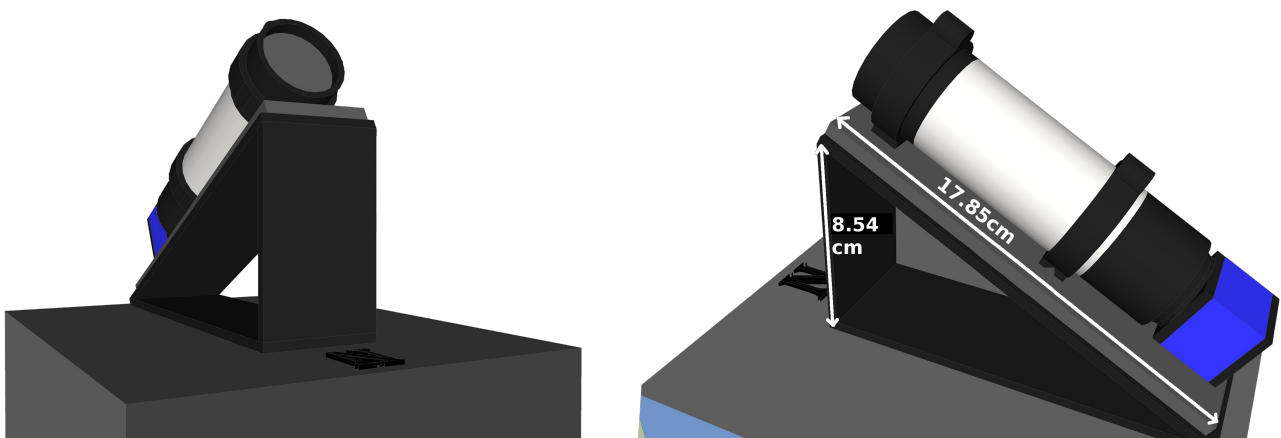


Figura 12. Detailed design of the device. The blue box corresponds to the CCD camera and the white cylinder to the telescope.

One of the most important facts about this design, which can be seen as a first working prototype in figure 13, is the lack of degrees of freedom: the telescope is absolutely fixed to the angled platform by a series of screws and clamps that make all kinds of movements impossible; the platform itself is attached to the base (tripod or ground) by screws or the previously mentioned system of slots so the position of the whole device is completely established.



Figure 13. Photograph of the working device during one of the observational sessions.

4.3. Methodology.

By using the previously described device, the CCD camera can take pictures of a single region of the sky, the one around the NCP. The visual field appearing in the photographs should always be the same, as long as the surroundings of the device remain unaltered. This way, in case of perceiving any difference in the field of view, the only possible explanation is that the device itself has moved as a consequence of a crustal movement. Figure 14 shows a simulation of the expected results for different deformation values, as well as the ground deformation quantification method that is to be

used in this work. After the fitting function is found, every crustal displacement can be linked to a specific change in the CCD images and, consequently, it will be possible to infer crustal deformation values from the visual displacements showed in the photographs.

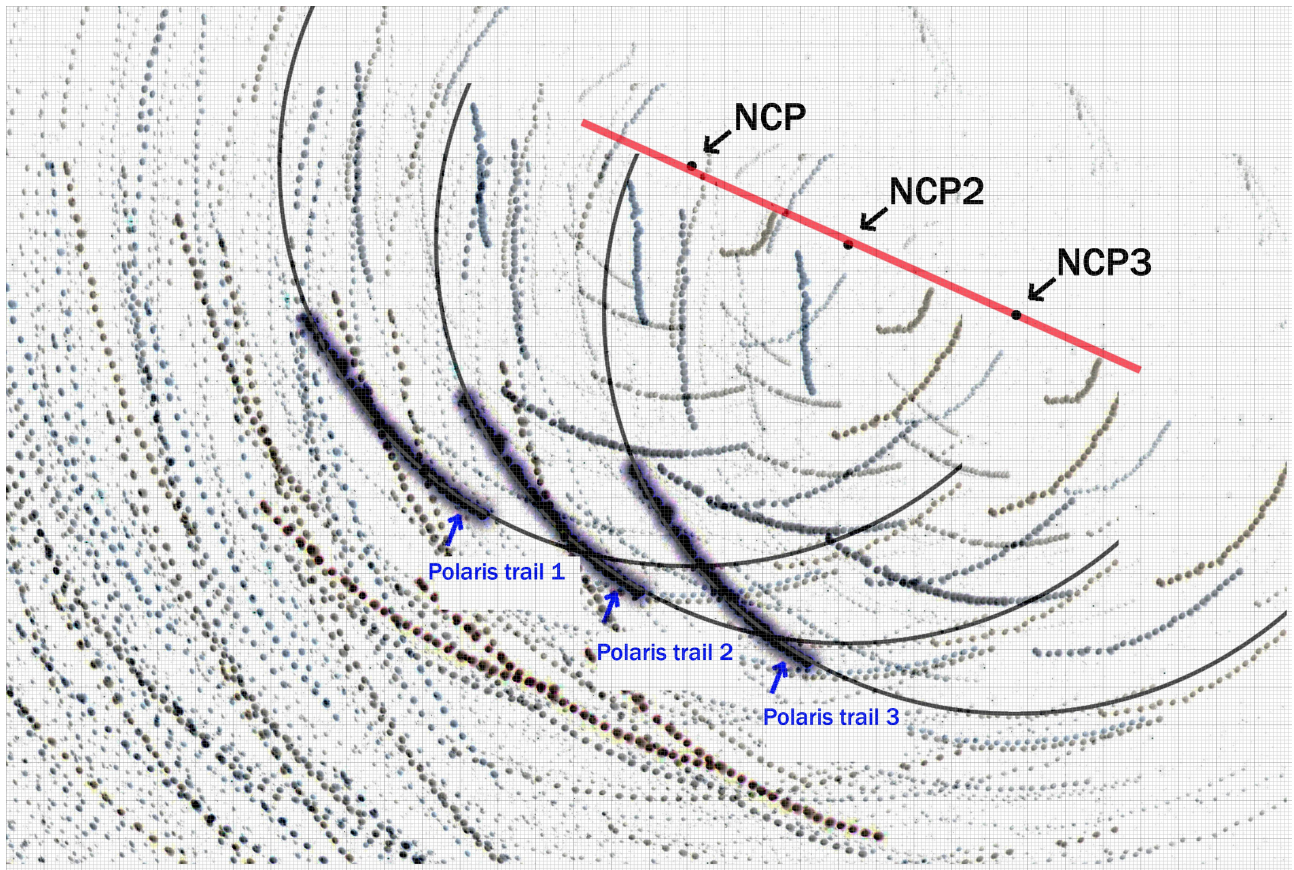


Figure 14. Composition of three different sequences for three different simulated positions of the device. After each sequence, the platform under the telescope is displaced, so the NCP would experience a deviation from its original position (NCP1). The circles represent the movement of the stars around the NCP, being the thick black line the one corresponding to the North Star. The aim of this method is to measure the NCP's displacement and to find a correlation between it and the corresponding crustal deformations.

5. Preliminary results.

Una vez se dispuso de un prototipo del dispositivo propuesto, se planificó una serie de observaciones a fin de comprobar si era posible inferir valores de deformaciones del terreno a partir del campo visual registrado por la cámara CCD. A tal fin, se desplazó el dispositivo al Observatorio del Teide y se tomó, a modo de comienzo, una serie de fotografías de 2 horas de duración del campo en torno a la posición inicial del PNC. A continuación, se elevó la base sobre la que se asientan el telescopio y la CCD 1mm y se realizó una nueva serie de fotografías de la misma duración. Este procedimiento se repitió dos veces más a lo largo de la sesión de observación, obteniéndose así cuatro series de fotografías denominadas PNC0, PNC+1, PNC+2 y PNC+3. Los resultados finales se muestran en la figura 16, la cual permite apreciar cómo deformaciones del terreno incluso menores de 1mm causan cambios lo suficientemente grandes en el campo de visión de la CCD, confirmando así la posibilidad de detectar deformaciones milimétricas y submilimétricas del terreno mediante el empleo de la geodesia astronómica.

Once the prototype was constructed and tested, an observational plan was established and carried out. First, a series of photographs were to be taken of the original or initial position of the NCP at the chosen location, the El Teide observatory. Figure 15a shows a composition of the images taken during a 2 hours interval and figure 15b the corresponding trajectories for some of the stars in the visual field.

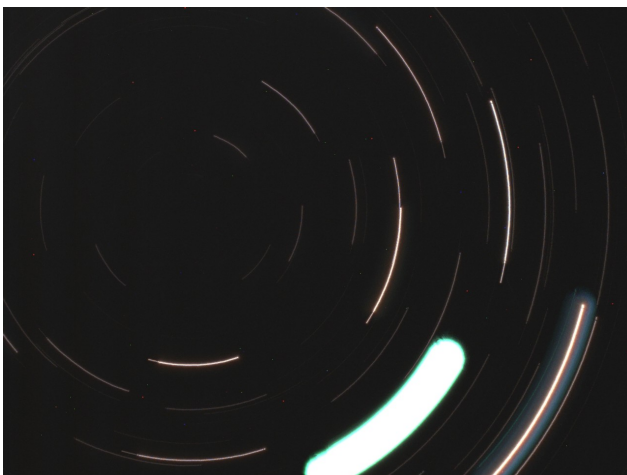


Figure 15a. Composition of a two hours photographic series showing the circular movement of the stars around the NCP.

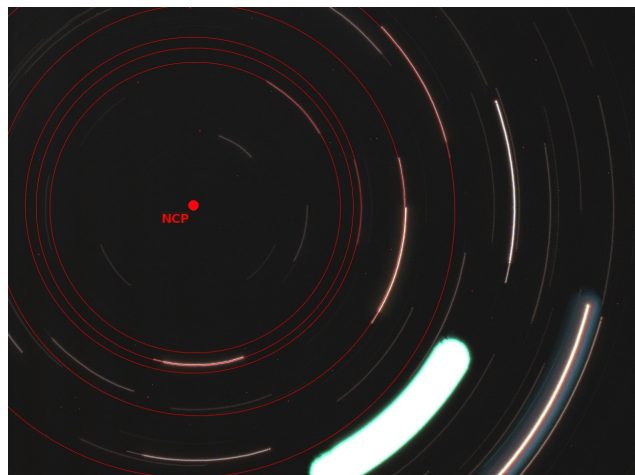


Figure 15b. Trails of some of the stars present in the visual field of the CCD camera and position of the NCP.

After the first series showed in figures 15a and 15b, the platform under the telescope and CCD camera was elevated 1mm before starting a new 2 hours photographic series. This procedure was repeated twice more, elevating the platform 1mm each time, so four different series, named NCP0, NCP+1, NCP+2 and NCP+3 were taken along the observational session. Figure 16 shows an overlapping composition of the four series in order to make it easier to compare and appreciate the differences in the results.

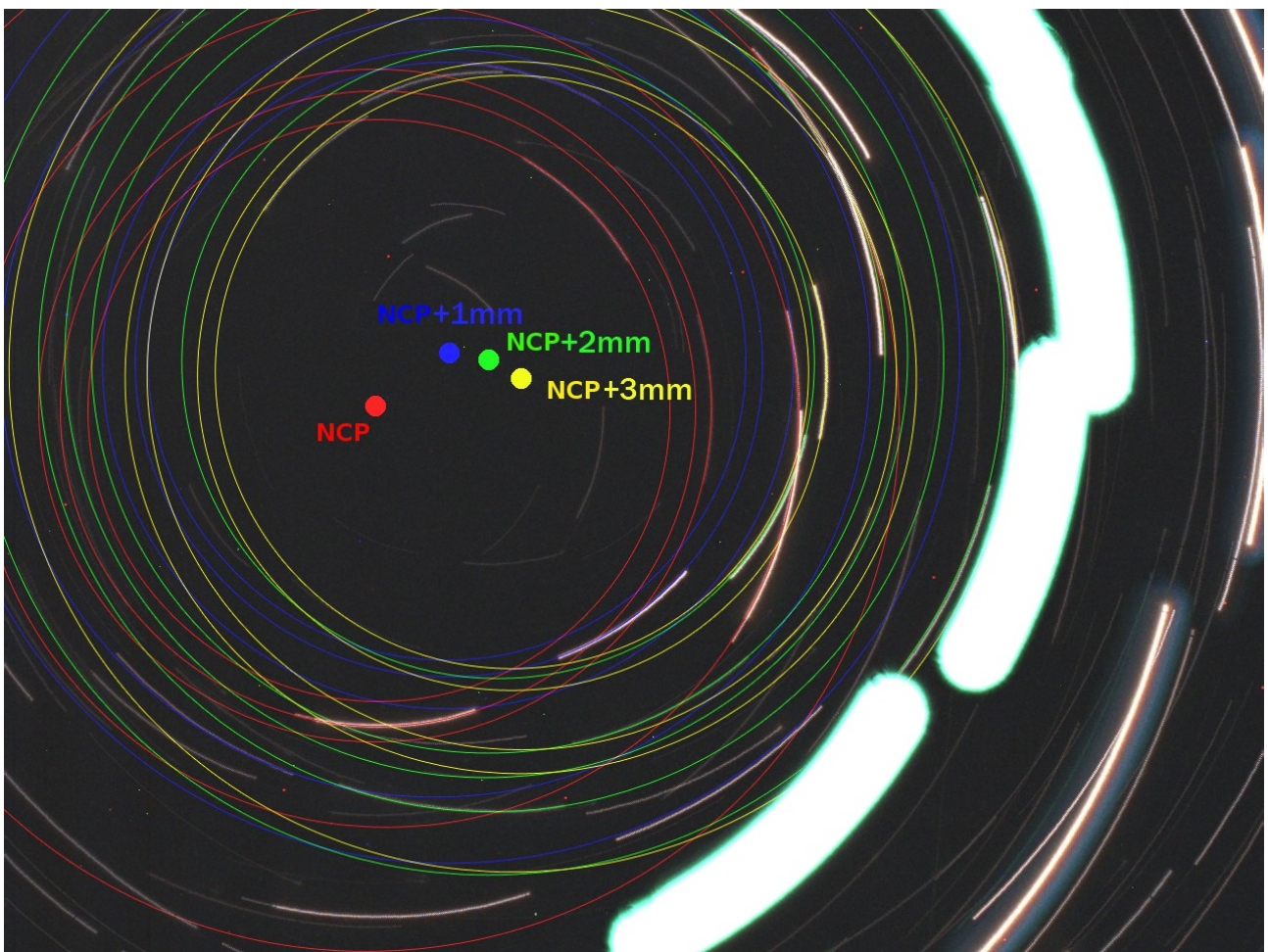


Figure 16. Overlap of the four different photographic series carried out during the observational session. Three different ground displacements were simulated (see text for details).

The results showed in the image above present the NCP positions for the four simulated ground deformations. It is to be noted that the unequal distance between the original NCP and the rest is probably caused by some small displacement of the tripod the device was mounted on during

the elevation of the platform under the telescope. As this was the first displacement to be performed, it was slightly more difficult to start it while the rest of them were considerably smoother.. The high sensitivity of the device along with the reduced visual field of the telescope are responsible of such large change in the position of the NCP.

In order to quantify the displacement suffered by the NCP in the images, the separation among the consecutive positions (in pixels) was measured, as showed in figure 17.

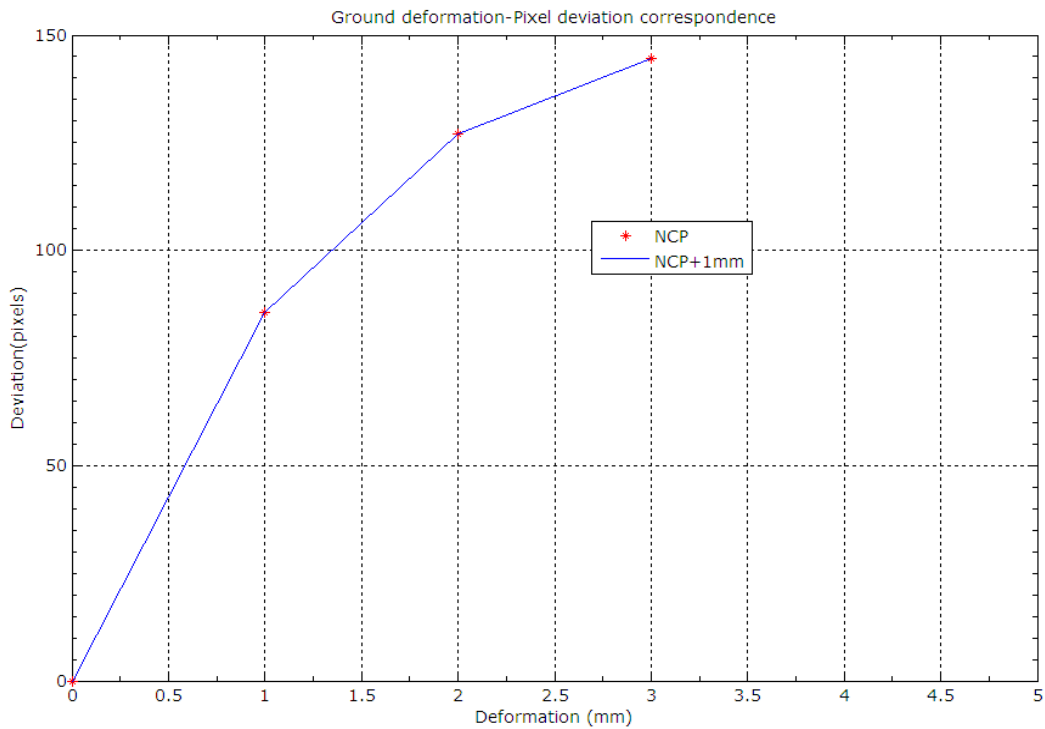


Figure 17. Correlation between the deformation simulated and the magnitude of the displacement of the NCP from its original position on the CCD's visual field.

No clear fitting function can be implied from this results, but they are the product of a single observational session with a mere prototype. Several sessions would be required with the definitive device in order to improve these results. However, the different series of tests carried out with this device generated satisfactory results for a 1mm crustal deformation. This would mean an estimate accuracy of at least 1mm, but it is to be expected to reach even better results after some more tests.

6. Conclusions and future works.

Las primeras pruebas realizadas en el terreno con el dispositivo propuesto arrojaron resultados satisfactorios que permitieron confirmar la posibilidad de determinar deformaciones del terreno con gran precisión (al menos del orden de 1mm) a partir de la variación de la posición del PNC en el campo de visión de la CCD. Las magnitudes de las deformaciones obtenidas en las simulaciones son todas superiores a este valor, por lo que el dispositivo propuesto en este trabajo sería capaz de detectarlas desde el observatorio.

Sin embargo, este montaje era sólo un prototipo inicial, montado sobre un trípode móvil, por lo que no permitía la comparación entre series de datos obtenidas en distintas sesiones de observación. El dispositivo final, con el que se espera contar en un futuro cercano, dispondría de una base estable y fijada al suelo, así como de un sistema de fijación permanente del telescopio a la cuña. Así, la mejora con respecto al prototipo (cuyo soporte era portátil) estaría en la posibilidad de hacer muchas series de pruebas de distinta duración, durante tantas noches como se deseara, a fin de comprobar los resultados obtenidos en este trabajo, comprobar si continúan obteniéndose al quitar y recolocar el instrumento de su posición sobre el soporte, definir de forma más precisa la posición inicial o estándar del PNC en el campo de la CCD y establecer el tiempo mínimo necesario para detectar su posición. Además, sería interesante realizar nuevas pruebas con un telescopio de mayor apertura que permitiera tener un mayor número de estrellas brillantes en su campo visual, con lo que se mejoraría el cálculo de la posición del PNC. Una vez montado y probado el dispositivo final, sería el momento de fijar un segundo punto de control/observación desde donde se repetirían las pruebas de localización del PNC y simulación de distintas deformaciones del terreno. En caso de obtener resultados igualmente satisfactorios, podría entonces desarrollarse una red alrededor de la isla con tantos puntos de control como se deseara.

Se está analizando además la posibilidad de construir la base y la plataforma mediante impresión 3D, ya que así se eliminaría cualquier grado de libertad del sistema y se abaratarían los costes, que resultarían considerablemente bajos en comparación con el de una estación GPS o un vuelo InSAR. Además de esto, es portátil, de pequeño tamaño, bajo peso y la CCD se alimenta a través del puerto USB de un ordenador corriente, por lo que la ya mencionada red que podría crearse en la isla podría ser controlada mediante un único dispositivo. Por último, también existe la posibilidad de automatizar el instrumento, mediante el empleo de una carcasa protectora, una fuente de energía y una antena, con las que podría controlarse a distancia. Aunque esto encarecería el dispositivo y ya no sería posible crear una red con una sola unidad del mismo, su coste seguiría

siendo más bajo que el de una estación GPS.

Este diseño tiene algunos inconvenientes, como el hecho de que únicamente funciona de noche y bajo condiciones meteorológicas favorables. Sin embargo, sus ventajas (sencillez, portabilidad, bajo coste y precisión) hacen de él una herramienta valiosa para completar la vigilancia volcánica de la isla.

The tests with the prototype generated satisfactory results and confirmed that it is possible to measure crustal deformations even smaller than 1mm by calculating the deviation of the NCP from its original position on the CCD visual field. Both GPS stations and InSAR techniques, which are the most employed techniques when measuring ground deformations, have accuracies up to 1cm, so the proposed device would improve greatly the current precision, making it possible to distinguish volcanic activity at an earlier stage than the other methods. The deformation magnitudes obtained from the dikes and magma chamber simulations are all larger than 1 mm at the observatory and, consequently, it is possible to establish that the proposed device is able to detect most cases of volcanic activity in Tenerife.

However, the instrument used on this work was just the initial prototype and, as it was mounted on top of a movable tripod, it was not possible to compare results obtained on different observational sessions. The definitive device would have a permanent and stable base and the telescope would be attached to the platform in an absolute way. Such an instrument would allow to do as many repetitions as needed (for as many nights as required) of the whole photographic series to confirm the results showed in this work, to check if the same values are obtained once the device is removed from its position and placed again on its base, to accurately establish the initial position of the NCP at the new location and the minimum required time to find it. Furthermore, it would be interesting to perform new tests with a telescope with a wider apparent field of view, as it would contain more stars (and possibly some more bright ones) and it would make it easier and more accurate to find the position of the NCP. Once the final device was settled and tested, it would be convenient to establish a second observational spot and make new repetitions of the previous tests in order to confirm the initial results. In case they were positive, a whole network around the island (or even around the archipelago) could be developed with as many control spots as desired.

The possibility of creating the final device by using a 3D printer is being studied, as it would

make it possible to have most part of it (base, platform and telescope tube) in a single piece, thus eliminating all degrees of freedom and making it cheaper. The cost of the device lies within a few hundred euros, being this significantly cheaper than GPS stations and the acquisition and analysis of InSAR imagery. In addition to this, the proposed instrument is portable thanks to its small size and light weight, and it is fed by the USB port of a regular computer. In the field, it only needs a stable base to be installed on, so a whole control network around the island (with as many stations as desired) could be created and operated with only one instrument.

This device has some disadvantages and limitations, as it only works during night-time and under favourable weather conditions. However, the peculiarities of its design (simplicity, portability, cheapness and accuracy) conform such an advantageous device that it can be considered a valuable complement to the existing volcanic activity surveillance methods.

REFERENCES

- Ablay, G., and Hurlimann, M. (2000), *Evolution of the north flank of Tenerife by recurrent giant landslides*, J. Volcanol. Geotherm. Res. 103, 135-139.
- Albert-Beltrán, J.F. Araña, V., Diez, J.L., and Valentín, A. (1990), *Physical-chemical conditions of the Teide volcanic system (Tenerife, Canary Islands)*, J. Volcanol. Geotherm. Res. 43, 321-332.
- Ancochea, E., Fúster, J.M., Ibarrola, E., Cendrero, A., Coello, J., Hernán, F., Cantagrel, J.M., and Jamond, A. (1990), *Volcanic evolution of the island of Tenerife (Canary Islands) in the light of new K-Ar data*, J. Volcanol. Geotherm. Res. 44, 231-249.
- Ancochea, E., Huertas, M.J., Cantagrel, J.M., Coello, J., Fúster, J.M., Arnaud, N., and Ibarrola, E. (1999), *Evolution of the Cañadas edifice and its implications for the origin of the Cañadas Caldera (Tenerife, Canary Islands)*, J. Volcanol. Geotherm. Res. 88, 177-199.
- Araña, V. (1985), *Evolución y mezcla de magmas en Las Cañadas del Teide. En Mecanismos eruptivos y estructuras profundas de volcanes italianos y españoles*. Reunión Cient. CSIC-CNR 38-42.
- Araña, V., Aparicio, A., García Cacho, L., and García García R. (1989), *Mezcla de magmas en la región central del Teide. En Los volcanes y la caldera del parque nacional del Teide (Tenerife, Islas Canarias)*, eds. V. Araña y J. Coello, 269-299.
- Araña, V., Camacho, A.G., García, A., Montesinos, F.G., Blanco, I., Vieira, R., and Felpeto, A. (2000), *Internal structure of Tenerife (Canary Islands) based on gravity, aeromagnetic and volcanological data*, J. Volcanol. Geotherm. Res. 103, 43-64.
- Bravo, T., Coello, J., and Bravo, J. (1976), *II Asamblea Nacional de Geodesia y Geofísica*, Madrid, Vol. Com. 2235-2244.
- Cabrera, M.P., and Hernández-Pacheco, A. (1987), *Las erupciones históricas de Tenerife (Canarias) en sus aspectos vulcanológico, petrológico y geoquímica*, Rev. Mat. Proc. Geol. V, 143-182.
- Carracedo, J.C., and Soler, V. (1983), *V Asamblea Nacional de Geodesia y Geofísica*, Madrid, Vol. Com. 2351-2363.
- Carracedo, J.C. (1994), *The Canary Islands: An example of structural control on the growth of large oceanic-island volcanoes*, J. Volcanol. Geotherm. Res. 60, 225-241.
- Carracedo, J.C., Paterne, M., Guillou, H., Perez Torrado, F.J., Paris, R., Rodriguez Badiola, E., and Hansen, A. (2003a), *Dataciones radiométricas (C14 y K/Ar) del Teide y el rift noroeste, Tenerife, Islas Canarias*, Estudios Geol. 59, 15-29.
- Carracedo, J.C., Guillou, H., Paterne, M., Pérez Torrado, F.J., Paris, R., and Badiola, E.R. (2003b), *Carbon-14 ages of the past 20 ka of eruptive activity of Teide volcano*, Canary Islands, EGS - AGU - EUG Joint Assembly, Abstracts from the meeting held in Nice, France, 6 - 11 April 2003, abstract #2627.
- Diez, J.L., and Albert, J.F. (1989), *Modelo termodinámico de la cámara magmática del Teide. En Los volcanes y la caldera del parque nacional del Teide (Tenerife, Islas Canarias)*, eds. V. Araña y J. Coello, 335-343.

-Eff-Darwich A., Grassin O., Fernández J. (2008). *An upper limit to ground deformation in the island of Tenerife, Canary Islands, for the period 1997-2006*. Pure and Applied Geophysics, 165,nº6 1049-1070.

-Eff-Darwich A., García-Lorenzo B., Rodríguez-Losada J.A., de la Nuez J., Hernández-Gutiérrez L.E., Romero-Ruiz M.C. (2009). *Comparative analysis of the impact of geological activity on astronomical sites of the Canary Islands, Hawaii and Chile*. Mon. Not. R. Astron. Soc. 000.

-Farrujia, I., Delgado, P., and Bethencourt, J. (1994), *Congr. Análisis y Evolución de la Contaminación de las Aguas Subterráneas*, Alcalá de Henares, Tomo II 397-416.

-Feigl, K.L., Dupré, E. (1998), *RNGCHN: a program to calculate displacement components from dislocations in an elastic half-space with applications for modeling geodetic measurements of crustal deformations*, Computers & Geosciences 25 (1999) 695-704 .

-Fernandez et al. (2003). *New geodetic monitoring system in the volcanic island of Tenerife, Canaries, Spain. Combination of InSAR and GPS techniques*. Journal of Volcanology and Geothermal Research 124.

-Guillou, H., Carracedo, J.C., Paris, R. and Pérez Torrado, F.J. (2004), *Implications for the early shield-stage evolution of Tenerife from K/Ar ages and magnetic stratigraphy*, Earth Planet. Sci. Lett. 222, 599-614.

-Hernández, P.A., Pérez, N.M., Salazar, J.M., Nakai, S., Notsu, K., and Wakita, H. (1998), *Diffuse emission of carbon dioxide, methane, and helium 3 from Teide volcano, Tenerife, Canary Islands*, Geophysical Research Letters 25, 3311-3314.

-Luis, J.F. (2007) *Mirone: A multi-purpose tool for exploring grid data*. Computers & Geosciences, 33, 31-41.

-Martí, J., Mitjavila, J., and Araña, V. (1994), *Stratigraphy, structure and geomorphology of the Las Cañadas Caldera (Tenerife, Canary Islands)*, Geol. Mag. 131, 715-727.

-Pérez, N.M., Nakai, S., Wakita, H., Hernández, P.A., and Salazar, J.M. (1996), *Helium-3 emission in and around Teide volcano, Tenerife, Canary Islands, Spain*, Geophysical Research Letters 23, 3531-3534.

-Valentín, A., Albert-Beltrán, J., and Diez, J. (1990), *Geochemical and geothermal constraints on magma bodies associated with historic activity, Tenerife (Canary Islands)*, J. Volcanol. Geotherm. Res. 44, 251-264.

